X-ray emission from stainless steel foils irradiated by femtosecond petawatt laser pulses

IOP Conf. Series: Journal of Physics: Conf. Series **946** (2018) 012018 doi:10.1088/1742-6596/946/1/012018

X-ray emission from stainless steel foils irradiated by femtosecond petawatt laser pulses

M A Alkhimova[2,3], A Ya Faenov[1,2], T A Pikuz[2,4], I Yu Skobelev[2,3], S A Pikuz[2,3], M Nishiuchi[5], H Sakaki[5], A S Pirozhkov[5], S Sagisaka[5], N P Dover[5], Ko Kondo[5], K Ogura[5], Y Fukuda[5], H Kiriyama[5], T Esirkepov[5], S V Bulanov[5], A Andreev[6,7], M Kando[5], A Zhidkov[8], K Nishitani[9], T Miyahara[9], Y Watanabe[9], R Kodama[1,4,8] and K Kondo[5]

[1] Institute for Academic Initiatives, Osaka University, 1-1 Yamadaoka, Suita, Osaka 565-0871, Japan
[2] Joint Institute for High Temperatures of the Russian Academy of Sciences, Izhorskaya 13 Bldg 2, Moscow 125412, Russia
[3] National Research Nuclear University MEPhI (Moscow Engineering Physics Institute), Kashirskoe Shosse 31, Moscow 115409, Russia
[4] Graduate School of Engineering, Osaka University, 2-1, Yamadaoka, Suita, Osaka 565-0871, Japan
[5] Kansai Photon Science Institute, National Institutes for Quantum and Radiological Science and Technology, Kizugawa-shi 8-1-7, Umemidai, Kyoto 619-0215, Japan
[6] Max Born Institute, Max-Born-Straße 2A, Berlin 12489, Germany
[7] Extreme Light Infrastructure—Attosecond Light Pulse Source, Dugonics 13, Szeged 6720, Hungary
[8] Photon Pioneers Center, Osaka City University, 2-1 Yamadaoka, Suita, Osaka 565-0871, Japan
[9] Interdisciplinary Graduate School of Engineering Sciences, Kyushu University, 6-1 Kasugakoen, Kyushu, Fukuoka 816-8580, Japan

E-mail: `maalkhimova@mephi.ru`

Abstract. We report about nonlinear growth of x-ray emission intensity emitted from plasma generated by femtosecond petawatt laser pulses irradiating stainless steel foils. X-ray emission intensity increases as $\sim I^{4.5}$ with laser intensity I on a target. High spectrally resolved x-ray emission from front and rear surfaces of 5 μm thickness stainless steel targets were obtained at the wavelength range 1.7–2.1 Å, for the first time in experiments at femtosecond petawatt laser facility J-KAREN-P. Total intensity of front x-ray spectra three times dominates to rear side spectra for maximum laser intensity $I \approx 3.2 \times 10^{21}$ W/cm^2. Growth of x-ray emission is mostly determined by contribution of bremsstrahlung radiation that allowed estimating bulk electron plasma temperature for various magnitude of laser intensity on target.

1. Introduction

Recent years petawatt laser (PWL) facilities become available in several laboratories worldwide. PWLs allow to study various issues of particle beams acceleration [1–4] simulate astrophysical phenomena in laboratory conditions [5, 6] and create extremely bright short x-ray sources [7, 8].

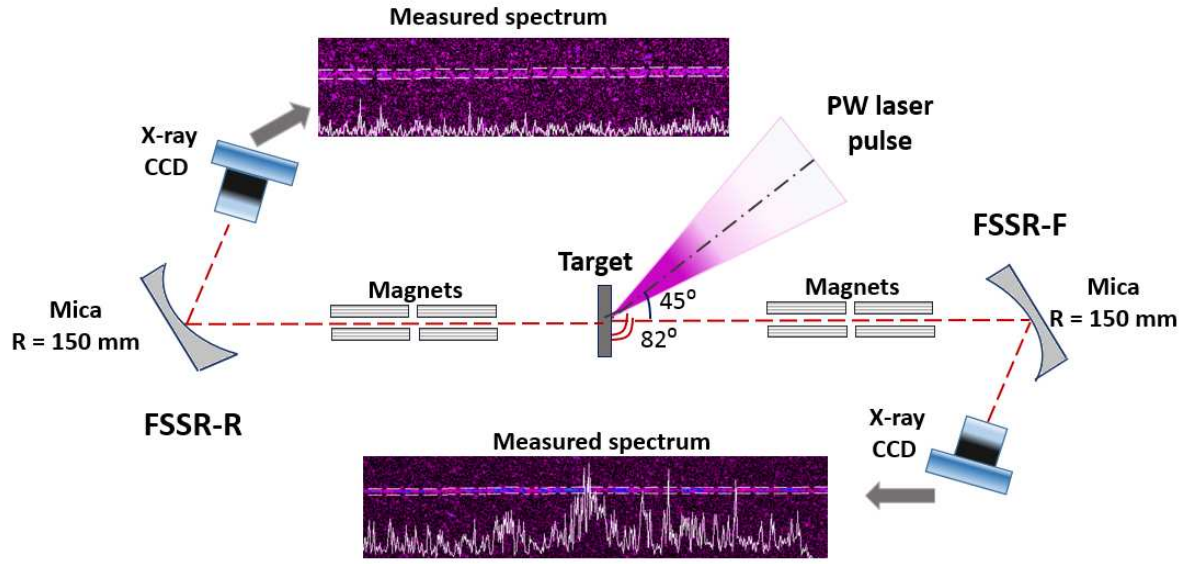

Figure 1. Experimental setup. Laser beam is focused on the foil surface at the angle 45° to create plasma. Generated plasma emitted x-ray radiation measured by two x-ray spectrometers installed at front and rear sides of target surface about 20 degree above the laser radiation plane. The spectrometers are equipped with mica spherical crystals, permanent magnet slits and Andor x-ray CCD detectors.

Correspondingly dense plasma created by femtosecond PWL pulse irradiation of a thin-foil target was continually considered as a powerful x-ray source [9–11].

The idea of ultra-bright x-ray generation in PWL experiments is as follows. Ultra-intense laser pulse focused onto thin metal foil creates highly ionized plasma at the laser focal spot. Due to optical field ionization valence electrons are quickly accelerated up to MeV energies. Such electrons multiply passing through the target emit x-ray photons up to high energies. These x-ray photons irradiate peripheral target area that results in heating and inner-shell transition pumping in atoms or ions, and hollow atoms excitation as a consequence [9, 12]. Hollow atom emission lines could be applied for determination of powerful x-ray radiation source parameters [13]. It was shown in [11] and [14] that for hollow ions emission appearance in x-ray spectra of elements with $Z \sim 10$, x-ray pumping power has to be higher than $I_{\text{x-ray}} \sim 10^{17}$ W/cm^2.

In general, laser intensity increase should results in x-ray intensity growth but in practice laser intensity is rather limited due to complexity of laser facility construction, laser energy transport losses and optic aberrations. As was previously described, the growth of x-ray source intensity has non-liner dependence on laser pulse energy expressed as $\sim E^n$ where $n \approx 4$–5 [11]. The most common way to study the dependence on laser intensity in experiment is to vary the focusing of laser beam on a target. The influence of laser focusing on x-ray emission intensity from dense plasma generated by high-Z foils irradiated by femtosecond laser pulses possesses remarkable interest. In this paper we consider how x-ray yield from stainless steel (SUS) depends on the magnitude of laser intensity on the target surface. We compare x-ray emission obtained from both sides of the target and contained highly spectrally resolved K-shell and bremstrahlung radiation.

2. Experimental set-up: Measurements of x-ray spectra

The measurements were made at the J-KAREN-P facility, which is optical parametric chirped-pulse amplification (OPCPA) Ti: Sapphire hybrid laser system at Kansai Photon Science Institute [15]. Laser pulses with duration of 40 fs (full width at half maximum, FWHM, with respect to intensity) and wavelength of 0.8 μm focused onto target by f/1.4 off-axis parabolic mirror at an incidence angle of 45° producing $d = 1.5$–2 μm (FWHM measurements) focal spot. Laser energy on target reached ≈ 10 J that corresponds to maximum laser-peak intensity $I \sim 3.2 \times 10^{21}$ W/cm^2. The intensity on target is varied by shifting the position of the target along the laser beam axis, changing the focal spot size. To register x-ray emission from SUS foil-targets of 5 μm thickness radiated by femtosecond PWL pulses two x-ray focusing spectrometers with high spectral resolution (FSSR) were implemented (see figure 1 for setup).

X-ray spectrometers were installed in front side (irradiated by laser pulse) and rear side of the target surface, at the distance $L = 2600$ and 1900 mm from plasma respectively. Both spectrometers were equipped with spherically bent mica crystals (curvature radius $R = 150$ mm, lattice spacing 19.94 Å). These crystals were aligned to register K-shell emission spectra of multi-charged (He_α line of Fe XXV and Ly_α line of Fe XXVI) and neutral (i.e. K_α, K_β lines) Fe ions in the wavelength range 1.6–2.1 Å. However, mica crystal ability to reflect radiation in different reflection orders leads to appearance of intense neutral Cr K_α line and Fe K_α line from 7^{th} and 8^{th} reflection orders simultaneously (figure 2). X-ray emission from 1^{st} to 5^{th} reflection orders has been attenuated by 100 μm Mylar ($C_{10}H_8O_4$) films located in front of the crystals to protect from debris pollution. X-ray spectra were measured by an x-ray Andor DX420 back-illuminated charged coupled device (CCD) with 26 μm pixel size. CCD apertures were protected against exposure to visible light using 2 layers of 1 μm thick polypropylene coated both sides with 0.2 μm Al. X-ray emission observed from front and rear sides of the target surface for various target positions offset from the best focus position are shown in figure 2. Raw x-ray spectra were averaged over three shots to increase signal-to-noise ratio. By changing the target position along the laser axis we varied laser intensity on target surface keeping the laser energy on target $E_{\text{lt}} \approx 10$ J for all shots. Figure 2 shows that at maximum laser intensity He-like transitions of Fe predominate in front side spectrum, while in rear side spectrum Fe He_α lines appears to be of very low intensity, and Cr He_α and neutral Fe K_α lines keep recognizable intensities only. The short shift of the target to $l_f \sim 10$ μm from the best focus position leads to a distinguishable changes in both the spectra and x-ray yield. For such focusing position the total intensity of front side x-ray spectrum in the spectral range 1.6–2.1 Å decreases more notably than rear side spectrum intensity (figure 4). Meanwhile Cr He_α line has already disappeared in rear side spectrum while Fe He_α and Cr He_α stay dominant in front side spectrum. At further laser intensity lowering mostly neutral K_α and K_β transitions in Fe and K_α line in Cr ions are observed from both sides of the target.

In order to reveal the change in actual laser intensity regarding the target displacement, the intensity distribution across the attenuated laser beam was carefully measured in different cross sections using optical microobjective technique. Data examples are shown in figure 3 demonstrating the achievement of $\approx$ 2 μm tight focusing conditions in the case of zero displacement, and approximately 6 μm at FWHM focal spot diameter at +100 μm away from the best focus. The obtained dependence of the laser intensity regarding the target displacement is given in figure 3(c). From here it can be seen that just a 20 μm target displacement leads to 3 times laser intensity decrease, due to a sharp focusing with f/1.4 off-axis parabolic mirror. However, along $\sim$ 100 μm displacement range the laser intensity decreases rather slowly than it might be expected from general consideration for f/1.4 focusing system, demanding further studies.

X-ray yield was measured by the integration of FSSR data over the full observation range covering 1.7 to 2.1 Å: wavelength band. Using the data on laser focusing conditions described

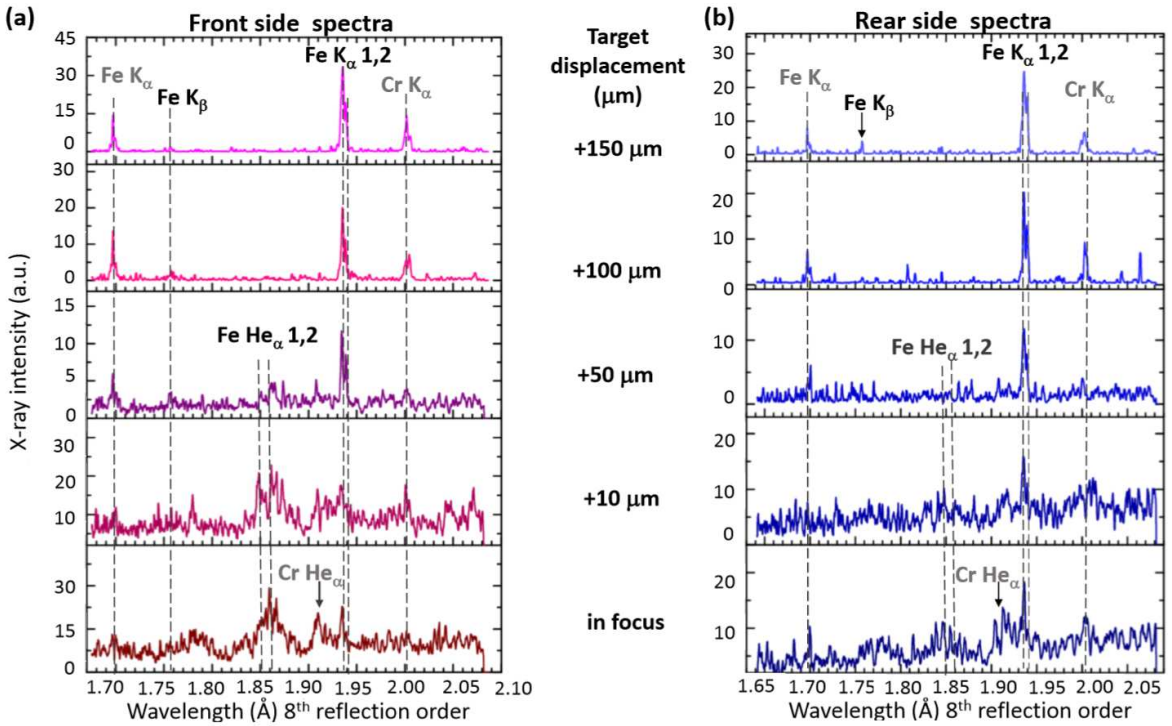

Figure 2. X-ray emission spectra from 5 μm SUS foils measured for various target displacement. (a) Front side x-ray spectra observed for laser energy on target $E_{\rm lt} \approx 10$ J and different magnitudes of laser intensity on target surface. (b) Corresponding rear side spectra measured in same shots.

Table 1. Bulk electron temperature estimation for the 2×10^{20} to 3×10^{21} W/cm^2 range of laser intensities on target. Temperature estimation is made with the assumption of bremsstrahlung radiation to be registered from 5$^{\rm th}$ and 7$^{\rm th}$ mica reflection orders.

Target displacement l_f (μm)	Laser intensity on target (10^{21} W/cm^2)	Front side $T_{\rm e}$ (eV)	Rear side $T_{\rm e}$ (eV)
0	3.2	850	450
10	2.7	780	400
50	0.9	320	210
100	0.4	160	160
150	0.23	140	140

above, the dependence of x-ray yield from in SUS 5 μm target was obtained versus the laser intensity. Figure 4 shows that x-ray yield, as seen both from the front and the rear side of the target foil, is quite sensitive to the laser intensity, especially in the range of $I \approx (1\text{–}3)\times10^{21}$ W/cm^2 intensities. From here it can be revealed that x-ray emission intensity $I_{\text{x-ray}}$ increases with laser intensity as $I_{\text{x-ray}} \sim I_{\rm lt}^{4.5}$ and $I_{\rm lt}^{3.5}$ for front and rear sides of target respectively, where $I_{\rm lt}$ is the magnitude of laser intensity on target.

The contribution of continuum radiation brightly observed in the spectra measured near the focus ($l_f \approx 0 \pm 10$ μm) becomes very weak at $l_f \sim 100$ μm and further. This probably could be

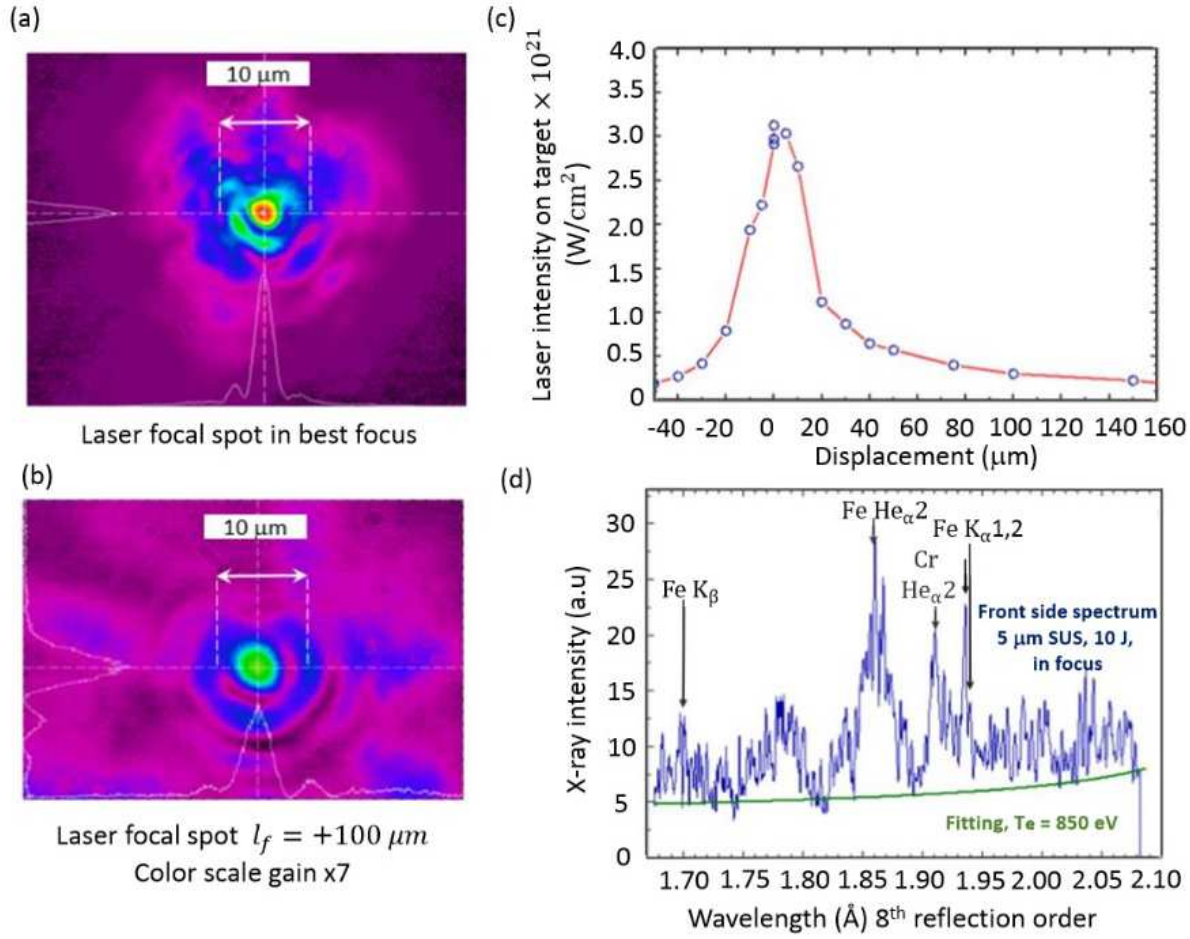

Figure 3. Focal spot image obtained for the best focusing displacement along the laser axis $l_f = 0$ (a) and $+100$ μm (b). (c) Laser intensity on the target vs target displacement. Laser intensity calculation include the focal spot size measurements data for various l_f and laser pulse duration $\tau \sim 40$ fs. (d) X-ray spectra measured at best focusing conditions, and bulk electron temperature estimation with the assumption of bremsstrahlung radiation contribution in measured x-ray spectra.

attributed to the lowering of collisional processes efficiency. This assumption allows estimating bulk plasma electron temperature by determination of bremsstrahlung radiation contribution to the measured spectra.

Bremsstrahlung spectrum is given as $I_{\rm brs} \sim A \exp^{-12.4/(\lambda T_{\rm e})} /(\lambda^2)$, where λ is the wavelength (Å), $T_{\rm e}$ is the bulk electron temperature (keV), A is a constant. The measured x-ray spectra (see i.e. figure 3) was fitted to estimate $T_{\rm e}$ for different laser intensities on target given in table 1 along with the revealed laser intensities for the particular target displacements. It is necessary to notice a certain roughness in such bulk temperature estimation allowing to determine $T_{\rm e}$ values not better than with 20% accuracy (140 ± 30 eV) for the lowest electron temperature. Plasma generated at the front side target surface has the bulk electron temperature $T_{\rm e} \approx 850$ eV for maximum laser intensity $I \approx 3.2 \times 10^{21}$ W/cm^2 while rear side plasma temperature $T_{\rm e}$ is of ≈ 450 eV. For lowest studied laser intensities $I \approx 2.3 \times 10^{20}$ W/cm^2. The bulk plasma temperature was of ≈ 140 eV.

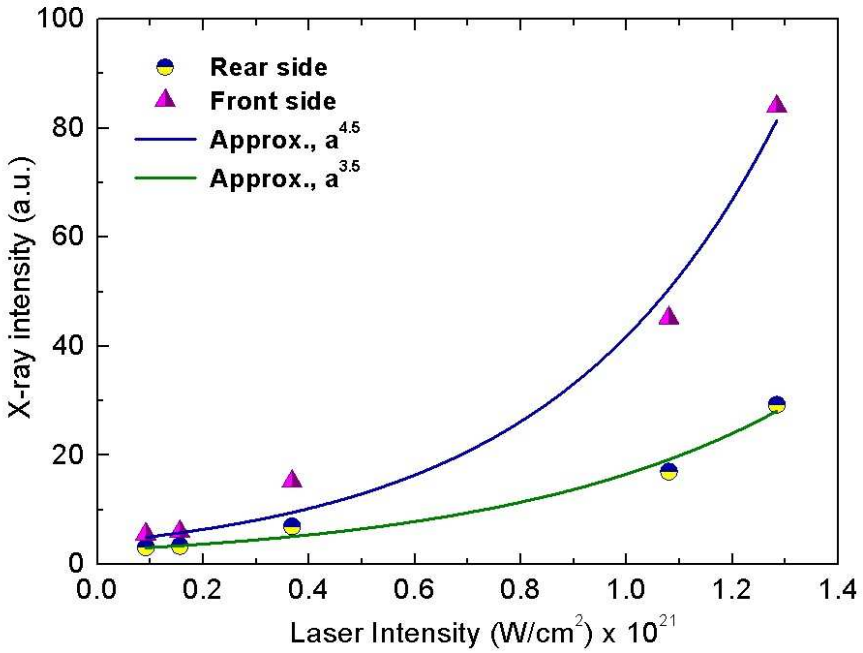

Figure 4. Total x-ray emission intensities as a function of different laser intensities on target. Intensity of x-ray emission integrated over the wavelength range 1.7–2.1 Å.

3. Conclusion

We demonstrated that x-ray yield in the range from 1.7 to 2.1 Å from femtosecond-duration-PWL-produced plasma is sensitive to the laser intensity on target ranged from 2×10^{20} to 3×10^{21} W/cm^2 and increases as $I_{\text{x-ray}} \sim I_{\text{lt}}^{4.5}$. X-ray emission measured by front side spectrometer was three times more intense than rear side for maximum laser intensity. The difference could be explained by different bulk electron temperatures T_{e}. The estimated values of T_{e} are indicative for plasma created in full plasma area including the peripheral target region [11, 14]. Peripheral target region was heated to high electron temperatures keeping solid density by x-ray pumping or hot electrons from focal spot region. Meanwhile in the case of SUS targets the plasma temperature in the focal spot region could reach $T_{\text{e}} \approx 1700$ eV, as was required for Fe and Cr He-like transition excitation [3, 16]. Though the measured x-ray emission spectra for both front and rear sides of the target displayed no hollow atom transition lines, x-ray source $I_{\text{x-ray}} \sim 10^{17}$ W/cm^2 [11] should be formed in the central plasma region. However, such high intensities are appeared to be not enough effective to pump deep lying electrons in iron and chrome atoms, and to create significant populations of hollow atom states.

Acknowledgments

X-ray diagnostics and data analysis were made at JIHT RAS under financial support from the Russian Science Foundation, grant No. 14-50-00124.

References

[1] Schwoerer H, Pfotenhauer S, Jäckel O, Amthor K U, Liesfeld B, Ziegler W, Sauerbrey R, Ledingham K W D and Esirkepov T 2006 *Nature* **439** 445–8
[2] Nishiuchi M *et al* 2015 *Phys. Plasmas* **22** 033107
[3] Gonzalez-Izquierdo B *et al* 2016 *Nat. Commun.* **7** 12891
[4] Daido H, Nishiuchi M and Pirozhkov A S 2012 *Rep. Prog. Phys.* **75** 056401

[5] Bulanov S V, Esirkepov T Z, Kando M, Koga J, Kondo K and Korn G 2015 *Plasma Phys. Rep.* **41** 1–51
[6] Chen H *et al* 2015 *Phys. Rev. Lett.* **114** 215001
[7] Weisshaupt J, Juvé V, Ku S, Holtz M, Woerner M, Elsaesser T, Ališauskas S, Pugžlys A and Baltuška A 2014 Table-top hard x-ray source driven by sub-100 fs mid-infrared pulses *Proc. 2014 Conf. Lasers and Electro-Optics (CLEO)—Laser Science to Photonic Applications* (San Jose, CA) pp 1–2
[8] Miaja-Avila L, O'Neil G C, Uhlig J, Cromer C L, Dowell M L, Jimenez R, Hoover A, Silverman K L and Ullom J N 2015 *Struct. Dyn.* **2** 024301
[9] Colgan J *et al* 2013 *Phys. Rev. Lett.* **110** 125001
[10] Shiraga H *et al* 2011 *Plasma Phys. Controlled Fusion* **53** 124029
[11] Faenov A Ya, *et al* 2015 *Sci. Rep.* **5** 13436
[12] Pikuz S A *et al* 2013 *High Energy Density Phys.* **9** 560–7
[13] Colgan J *et al* 2016 *Europhys. Lett.* **114** 35001
[14] Pikuz S A, Faenov A Ya, Fortov V E and Skobelev I Yu 2014 *Phys. Usp.* **57** 702–7
[15] Kiriyama H *et al* 2015 *IEEE J. Sel. Top. Quantum Electron.* **21** 232–49
[16] Stafford A, Safronova A S, Faenov A Ya, Pikuz T A, Kodama R, Kantsyrev V L, Shrestha I and Shlyaptseva V V 2017 *Laser Part. Beams* **35** 92–9